Chaotic Modeling and Simulation (**CMSIM**) **4: 253–264, 2015**

Lyapunov spectrum analysis of natural convection in a vertical, highly confined, differentially heated fluid layer

Zhenlan Gao[1,2,3], Berengere Podvin[2], Anne Sergent[1,2], and Shihe Xin[4]

[1] CNRS, LIMSI, UPR3251, BP 133, 91403, Orsay Cedex, France
(E-mail: gao@limsi.fr)
[2] Universite Pierre et Marie Curie - Paris 06, 4 Place Jussieu, 75252 Paris, Cedex 05, France
[3] Arts et Métiers ParisTech, 2 Boulevard du Ronceray, 49035 Angers Cedex 01, France
[4] CETHIL, INSA de Lyon, 69621 Villeurbanne Cedex, France

Abstract. We use Lyapunov spectrum analysis to characterize the dynamics of a single convection roll between two differentially heated plates. 3D numerical simulation is carried out in a highly confined periodic domain. As the Rayleigh number increases, the intensity of the convection roll displays chaotic features while the roll remains stationary. For still higher values of the Rayleigh number, the roll intermittently moves between two positions separated by half a wavelength. We use Lyapunov spectrum analysis to help determine the characteristics of the flow in both regimes. We show that although the largest Lyapunov exponent is positive on average, the most probable value of the short-time Lyapunov exponent is negative. We compute the flow eigenvectors associated with the strongest variations in the exponent in the chaotic and the intermittent case and identify the corresponding hydrodynamic modes of instability.
Keywords: Natural convection, Period-doubling bifurcations, crisis-induced intermittency, Lyapunov spectrum.

1 Introduction

Natural convection between two vertical plates maintained at different temperatures is an important prototype to model heat transfer in industrial applications, such as plate heat exchangers or solar panels. The properties of heat transfer are deeply influenced by the nature of the flow, which is typically turbulent. It is therefore of interest to study the onset of chaotic dynamics in these flows. The development of instabilities in a differentially heated cavities with adiabatic walls has been studied numerically for a few decades [1,2]. Earlier studies are mostly limited to 2D geometries and relatively low Rayleigh numbers regimes (steady, periodis, quasi-periodic) with a focus on primary instabilities. Recent studies focus on the fully turbulent nature of the natural

Received: 20 December 2014 / Accepted: 6 October 2015
 ISSN 2241-0503

convection flow at high Rayleigh numbers [3], which remains a challenge owing to the double kinetic and thermal origin of the fluctuations.

Our studies attempt to bridge the gap between the relatively ordered flow observed at low Rayleigh numbers and the fully turbulent flow at high Rayleigh numbers. To this end, we carried out the three-dimensional direct numerical simulation (DNS) of a fluid layer between two vertical, infinite, differentially heated plates and determined the different stages leading to chaos [4]. The flow is characterized by co-rotating convection rolls which grow and shrink over time and interact with each other in a complex fashion. Similar rolls have also been observed in tall cavities of high aspect ratio [5]. A useful model of the problem can be obtained by limiting the dimensions of the plates in order to study the dynamics of a single convection roll. A cascade of period-doubling bifurcations and a crisis-induced intermittency have been observed in the vertically confined domain [6]. The goal of this paper is examine how Lyanunov exponent analysis can help characterize the chaotic dynamics of the flow in such a configuration.

2 Configuration

We consider the flow of air between two infinite vertical plates maintained at different temperatures. The configuration is represented in Figure 1. The distance between the two plates is D, and the periodic height and depth of the plates are L_z and L_y respectively. The temperature difference between the two plates is ΔT. The direction x is normal to the plates, the transverse direction is y, and the gravity g is opposite to the vertical direction z.

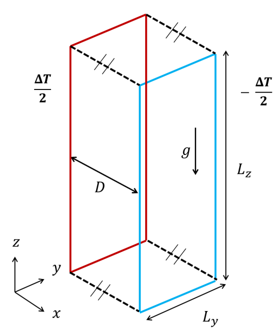

Fig. 1. (Color online) The simulation domain is constituted by two vertical plates, separated by a distance D and maintained at different temperatures. Periodic boundary conditions for the plates are enforced in both transverse and vertical directions (y and z). The aspect ratios of the periodic dimensions are $A_y = L_y/D = 1$ and $A_z = L_z/D = 2.5$. The temperature of the back plate at $x = 0$ (in red) is $\frac{\Delta T}{2}$, while that of the front plate at $x = 1$ (in blue) is $-\frac{\Delta T}{2}$. The distance between the plates is D.

The fluid properties of air, such as the kinetic viscosity ν, thermal diffusivity κ, and thermal expansion coefficient β, are supposed to be constant. Four nondimensional parameters characterizing the flow are chosen in the following way: the Prandtl number $\mathrm{Pr} = \dfrac{\nu}{\kappa}$, the Rayleigh number based on the width of the gap between the two plates $\mathrm{Ra} = \frac{g\beta\Delta T D^3}{\nu\kappa}$, and the transverse and vertical aspect ratio $A_y = L_y/D$ and $A_z = L_z/D$, respectively. Only the Rayleigh number is varied in the present study. The Prandtl number of air is taken equal to 0.71. The transverse aspect ratio is set to be $A_y = 1$, the vertical aspect ratio is set to $A_z = 2.5$, which corresponds to the critical wavelength $\lambda_{zc} = 2.513$ obtained by the stability analysis [4].

The flow is governed by the Navier-Stokes equations within the Boussinesq approximation. The nondimensional equations are:

$$\nabla \cdot \overrightarrow{u} = 0 \tag{1}$$

$$\frac{\partial \overrightarrow{u}}{\partial t} + \overrightarrow{u} \cdot \nabla \overrightarrow{u} = -\nabla p + \frac{\mathrm{Pr}}{\sqrt{\mathrm{Ra}}} \Delta \overrightarrow{u} + \mathrm{Pr}\theta \overrightarrow{z} \tag{2}$$

$$\frac{\partial \theta}{\partial t} + \overrightarrow{u} \cdot \nabla \theta = \frac{1}{\sqrt{\mathrm{Ra}}} \Delta \theta \tag{3}$$

with Dirichlet boundary conditions at the plates

$$\overrightarrow{u}(0, y, z, t) = \overrightarrow{u}(1, y, z, t) = 0, \quad \theta(0, y, z, t) = 0.5, \quad \theta(1, y, z, t) = -0.5 \tag{4}$$

and periodic conditions in the y and z directions. The equations (1)-(4) admit an $O(2) \times O(2)$ symmetry. One $O(2)$ symmetry corresponds to the translation in the transverse direction y and the reflection $y \to -y$, while the other corresponds to the translations in the vertical direction z and a reflection that combines centrosymmetry and Boussinesq symmetry: $(x, z, \theta) \to (1 - x, -z, -\theta)$.

A spectral code [7] developed at LIMSI is used to carry out the simulations. The spatial domain is discretized by the Chebyshev-Fourier collocation method. The projection-correction method is used to enforce the incompressibility of the flow. The equations are integrated in time with a second-order mixed explicit-implicit scheme. A Chebyshev discretization with 40 modes is applied in the direction x, while the Fourier discretization is used in the transverse and vertical directions. 30 Fourier modes are used in the transverse direction y for $A_y = 1$, while 60 Fourier modes are used in the vertical direction z for $A_z = 2.5$.

2.1 Description

For low Rayleigh numbers, the flow solution is laminar. A cubic velocity and linear temperature profile, which depend only on the normal distance from the plates are observed. The flow presents similar features to those of a confined mixing layer [9,4]. As the Rayleigh number Ra is increased, steady two-dimensional convection rolls appear at $\mathrm{Ra} = 5708$, which then at $\mathrm{Ra} = 9980$ become steady three-dimensional convection rolls linked together through braids of vorticity (see Figure 2). For still higher Rayleigh numbers, the flow becomes periodic at $\mathrm{Ra} = 11500$. The convection roll essentially grows and shrinks with a characteristic period of $T = 28$ convective time units, which is in good agreement with the natural excitation frequency of a mixing layer [9].

As the Rayleigh number increases, a series of period-doubling bifurcations appears, as illustrated in Figure 3. More details can be found in [6]. The onset of chaos was predicted to occur at Ra $\sim$ 12320, in agreement with numerical observations. The variations of the roll size become more disorganized and intense, but the position of the roll remains quasi-stationary. When Ra $= 12546$, the variations in the intensity of the roll become so large that the roll breaks down and reforms at another location, separated by half a vertical wavelength from the original one. In terms of dynamics this corresponds to crisis-induced intermittency, which can be seen in Figure 3(b). The difference between the chaotic and the intermittent regimes in terms of phase portraits is illustrated in Figure 4 for two Rayleigh numbers taken in each regime.

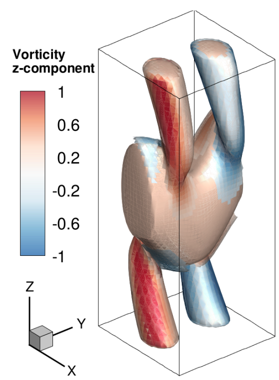

Fig. 2. (Color online) Q-criterion visualization of flow structures colored by the vertical vorticity Ω_z. Bi-periodic domain at Ra $= 12380$, $Q = 0.25$ in the present numerical configuration from Figure 1, i.e. with periodic boundary conditions in both y and z directions ($A_y = A_z = 1$);

3 Lyapunov spectrum

3.1 Definition

Several methods exist to distinguish between regular and chaotic dynamics in a deterministic system. The largest Lyapunov exponent, which measures the divergence rate of two nearby trajectories, is considered as a useful indicator to answer this question. Similarly, the n first Lyapunov exponents $\lambda_1 > \lambda_2 > \lambda_3 > ... > \lambda_n$ characterize the deformation rates of a n-sphere of nearby initial conditions. We applied the numerical technique proposed by Benettin *et al.* [8] to compute the Lyapunov spectrum of our fluid system, by parallelizing the DNS code described above with MPI library. On each processor, the flows are advanced independently in time. The flow on the processor-0 is the reference solution, which is obtained by numerical integration of the nonlinear equations. On the other processors, the randomly initiated perturbations $\delta\mathbf{X}$ are integrated in time by solving the linearized DNS code. The modified

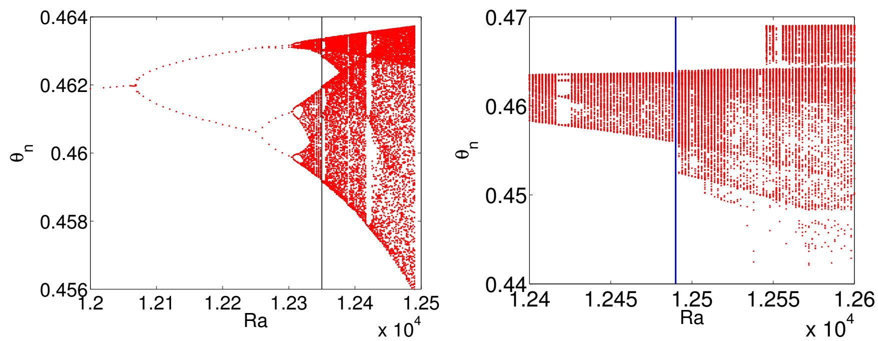

(a) (b)

Fig. 3. (Color online) Bifurcation diagram obtained by using the local maxima θ_n of the temperature time series at the point (0.038 0.097 0.983).Note: the vertical line in the figure corresponds the largest Rayleigh number in Figure 3 (a) $12000 < Ra < 12500$ (b) $12400 < Ra < 12600$.

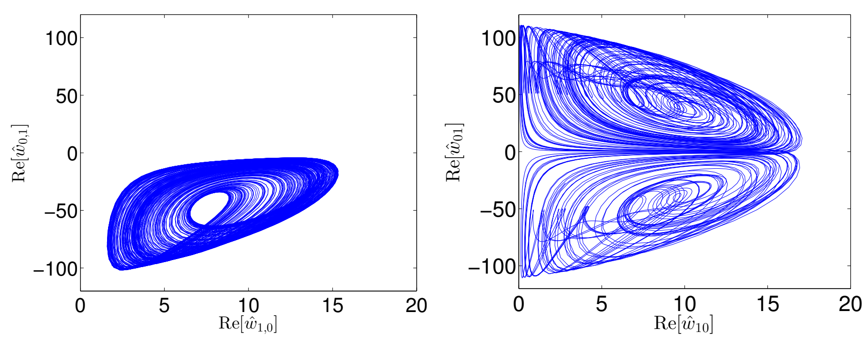

(a) Ra = 12380 (b) Ra = 12600

Fig. 4. (Color online) Phase portraits. Abscissa: real part of the the Fourier transform (in y and z) of the vertical velocity $\hat{w}_{01}(x)$ calculated on vertical plane $x = 0.0381$; ordinate: real part of the Fourier transform of the vertical velocity $\hat{w}_{10}$. (a) Ra = 12380, (b) Ra = 12600.

Gram-Schmidt procedure is applied every 20 time-steps of dt to renormalize the perturbations. At each renormalisation step, the instantaneous Lyapunov exponents were computed as

$$\lambda_i^{inst} = \frac{1}{\Delta t} \ln \frac{\|\delta \mathbf{X}(j\Delta t)\|_i}{\|\delta \mathbf{X}(0)\|_i} \tag{5}$$

Their asymptotic mean values form the long-time Lyapunov spectrum:

$$\lambda_i = \lim_{N\to+\infty} \frac{1}{N\Delta t} \sum_{j\in N} \ln \frac{\|\delta \mathbf{X}(j\Delta t)\|_i}{\|\delta \mathbf{X}(0)\|_i} \tag{6}$$

where λ_i is the i-th Lyapunov exponent and the norm mesuring the distance between two nearby trajectories is chosen as $\|\delta \mathbf{X}(t)\| = \sqrt{\int_V [\delta \overrightarrow{u}(t)^2 + \delta\theta(t)^2] dV}$.

3.2 Long-time Lyapunov exponents

The computation of Lyapunov spectrum for our fluid system was carried out at different Rayleigh numbers between Ra = 12360 and Ra = 12900. Errorbars for the Lyapunov exponent are estimated from the standard error of the mean assuming a Gaussian distribution and a 95% confidence interval. We note that the error on the exponent may be somewhat underestimated, as we do not take into account other sources of error, such as the distance to the attractor.

In all that follows, we focus on two Rayleigh numbers: one corresponds to the chaotic, non-intermittent system Ra = 12380. The other Ra = 12600 corresponds to a chaotic, intermittent case. Convergence tests were run for these two Rayleigh numbers Ra = 12380 and Ra = 12600 and two different time-discretizations $dt = 1 \times 10^{-3}$ and $dt = 1 \times 10^{-2}$. The 15 leading Lyapunov exponents are computed, among which the first 8 ones are listed in Table 1.

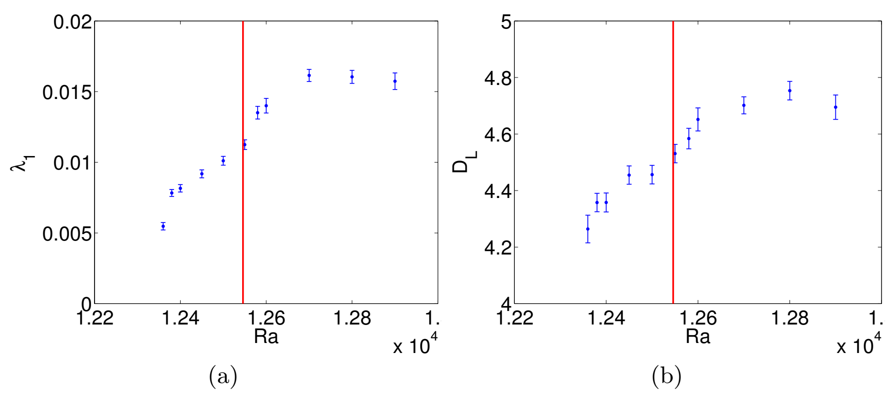

Fig. 5. (Color online) (a) The largest Lyapunov exponent λ_1 for different Rayleigh numbers; Error bars are 1.96 times the standard error. (b) Fractal dimension obtained by application of the Kaplan-Yorke formula as a function of the Rayleigh number. The position of the solid line spanning each figure represents the value of the Rayleigh number at the onset of the crisis.

As shown in Figure 3.2, the largest asymptotic Lyapunov exponent is positive for Ra $\geq$ 12360, and increases quasi-linearly for 12400 $<$ Ra $<$ 12546. This suggests that temporal chaos has been reached. For all Rayleigh numbers considered, only one single positive Lyapunov exponent is found and is on the order of 0.01. The test $0 - 1$ for chaos proposed by Gottwald and Melbourne [12,13] was applied to an appropriately sampled temperature time series, and returned a value close to 1, which confirms that our flow is chaotic. The Lyapunov exponent is considerably larger for the intermittent case Ra = 12600 than for the chaotic case Ra = 12380.

We find that the asymptotic value of exponents 2 to 4 is close to zero. We observe that the temporal oscillations of the short-time exponents 2 to 4 decrease with the time step, as can be expected. As shown by Sirovich and Deane [10] for Rayleigh-Bénard convection, three exponents should be zero:

Table 1. First 8 Lyapunov exponents at two different Rayleigh numbers for two different time steps.

	Ra = 12380		Ra = 12600	
λ_i	$dt = 1 \times 10^{-3}$	$dt = 1 \times 10^{-2}$	$dt = 1 \times 10^{-3}$	$dt = 1 \times 10^{-2}$
1	0.0094 ± 0.0004	0.0078 ± 0.0002	0.0199 ± 0.0005	0.0140 ± 0.0005
2	-0.00047 ± 0.00067	-0.00027 ± 0.00043	-0.0001 ± 0.0008	-0.0002 ± 0.0005
3	0.00075 ± 0.00048	0.00031 ± 0.00026	0.0036 ± 0.0006	0.0009 ± 0.0006
4	0.00010 ± 0.00053	-0.00090 ± 0.00031	0.00011 ± 0.00062	0.00047 ± 0.00066
5	-0.0579 ± 0.00020	-0.0220 ± 0.0001	-0.0594 ± 0.00017	-0.0230 ± 0.0001
6	-0.0726 ± 0.0006	-0.0485 ± 0.0004	-0.0696 ± 0.0006	-0.0464 ± 0.0006
7	-0.0709 ± 0.0006	-0.0318 ± 0.0004	-0.0732 ± 0.0006	-0.0328 ± 0.0006
8	-0.0843 ± 0.0006	-0.0571 ± 0.0004	-0.0919 ± 0.0006	-0.0594 ± 0.0006

one comes from the fact that the time derivative $\dfrac{\partial \mathbf{X}}{\partial t}$ of the reference solution $\mathbf{X}$ satisfies the linearized equation, since the system is autonomous. The other two zero exponents reflect the fact that $\dfrac{\partial \mathbf{X}}{\partial y}$, $\dfrac{\partial \mathbf{X}}{\partial z}$ also satisfy the linearized equation on account of the homogeneous boundary conditions.

All exponents of order $n \geq 5$ were found to be negative. Convergence was more difficult to reach for these higher-order exponents. However even if some uncertainty is present, this does not affect significantly the value of the fractal dimension.

The Lyapunov dimension was estimated using the Kaplan-Yorke formula [11]:

$$D_L = K + \frac{S_K}{|\lambda_{K+1}|} \tag{7}$$

where K is the largest n for which $S_n = \sum_{i=1}^{n} \lambda_i > 0$. It was found to be between 4.2 and 4.6, as can be seen in Figure 3.2 (b). An inflection point, corresponding to a sharp increase in the largest exponent, is observed at the onset of intermittency for both the largest exponent and the Lyapunov dimension.

4 Short-time Lyapunov exponent

As pointed out by Vastano and Moser [15], examination of the short-time Lyapunov exponent provides additional information about the flow. Figure 6 and 7 shows the distribution of the first Lyapunov exponent for the two Rayleigh numbers and the two time resolutions. We can see that the distributions are very similar for both time intervals, which shows the convergence of the computations. Corresponding time series of the largest Lyapunov exponent and their Fourier spectrum are represented in Figure 8. The fundamental excitation frequency $f = 0.22$ is dominant in the chaotic case. Lower frequencies become important in the chaotic case.

A striking fact is that for both Rayleigh numbers, although the mean value of the exponent is positive, the maximum value of probability distribution function (p.d.f.) is actually negative. This is markedly different from the results reported by Kapitaniak [14] for quasi-periodically forced systems, where the mean value of the exponent appeared to correspond to the maximum of the distribution. We note that no external forcing is imposed in our configuration, which is characterized by self-sustained oscillations. The distributions at Ra = 12380 and Ra = 12600 present many similarities. The main difference is that in the intermittent case the local maximum of the distribution for small positive values in Figure 6 disappears, while a band of significantly higher positive values (larger than 0.2) is created in Figure 7.

We computed the vector associated with local extrema of the short-time Lyapunov exponent which were identified in the time series. This gives us insight into the perturbations most likely to disorganize the flow. We checked that observations made at a particular time held for other times.

Results are presented in Figure 9 for the chaotic case. For the chaotic case, we have identified two types of relative extrema: (i) relatively small excursions, associated with the local maximum and the local minimum in the histogram from Figure 6 corresponding to positions marked with filled circles in Figure 8 (a). We find that the perturbation associated with a local maximum consists of almost 2D rolls (Figure 9 (a)), while the minimum corresponds to a strongly 3D flow and a relatively weaker convection roll (Figure 9 (b)). (ii) stronger excursions, where both extrema are associated with an essentially 2D flow (positions marked with filled squares in Figure 9 (c)(d)). 2D convection rolls correspond to the most unstable linear modes. However the convection rolls associated with maxima seem to be stronger than those associated with minima.

In the intermittent case, we focus exclusively on largest extrema. Figure 10 (a) shows that the maxima in time corresponds to a flow which is in fact almost 1-D (note the much lower value for the criterion $Q = 0.05$), while the minima in time corresponds to a 2D flow (see Figure 10 (b)). These two states can be associated with the break-up and formation of the roll.

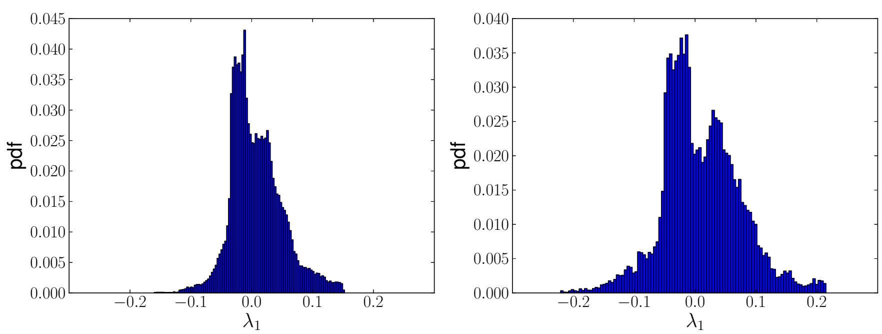

(a) $dt = 1 \times 10^{-2}$ (b) $dt = 1 \times 10^{-3}$

Fig. 6. (Color online) Probability distribution function (p.d.f.) of instantaneous 1st Lyapunov exponent λ_1^{inst} at Ra = 12380.

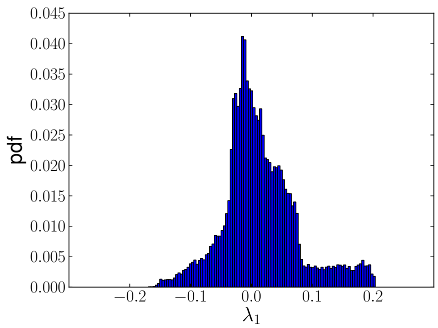

(a) $dt = 1 \times 10^{-2}$

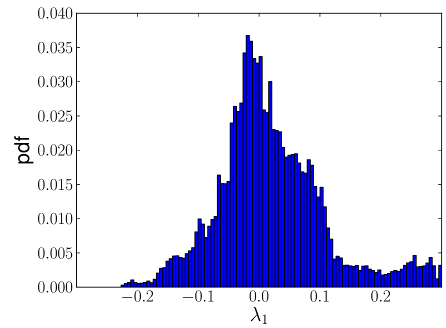

(b) $dt = 1 \times 10^{-3}$

Fig. 7. (Color online) Probability distribution function (p.d.f.) of instantaneous 1st Lyapunov exponent λ_1^{inst} at Ra = 12600.

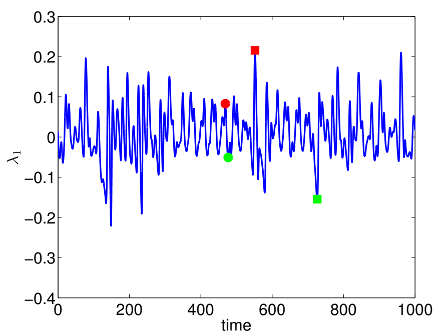

(a)

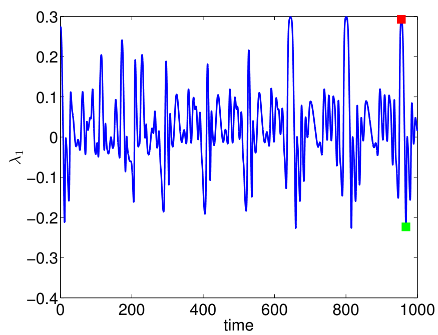

(b)

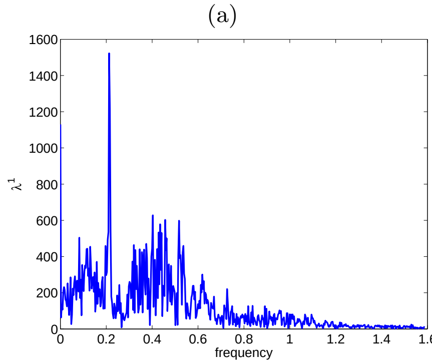

(c)

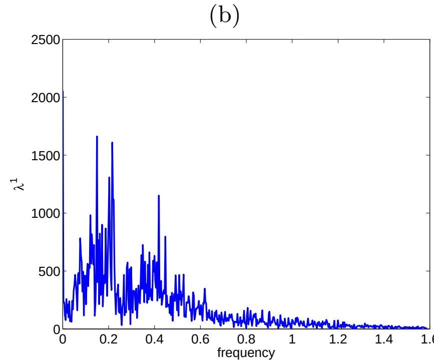

(d)

Fig. 8. (Color online) (a) (b) Evolution of the largest short-time Lyanunov exponent λ_1^{inst} at (a) Ra = 12380 (b) Ra = 12600; (c) (d) Temporal Fourier spectrum of the largest short-time exponent λ_1^{inst} at (c) Ra = 12380 (d) Ra = 12600.

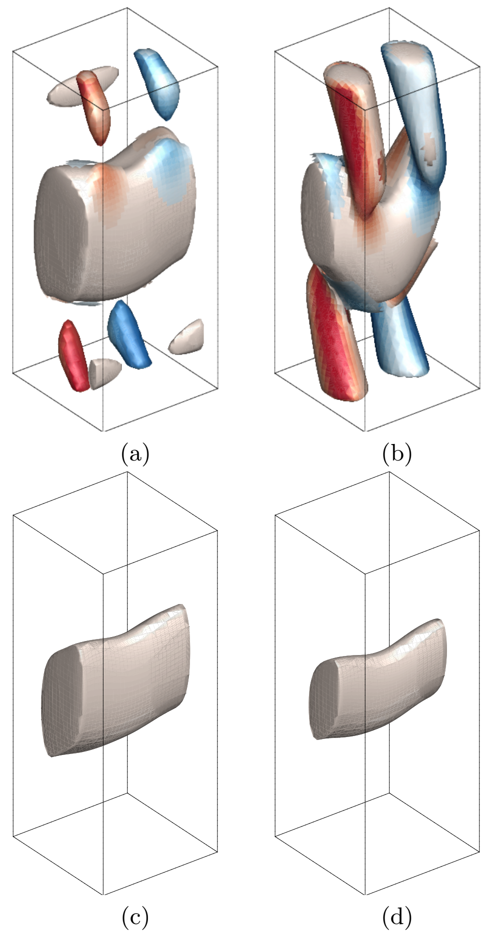

Fig. 9. (Color online) Eigenvector associated with a local extremum of the short-time exponent at Ra = 12380 at the positions indicated in Figure 8 (a). Value of the Q isosurface $Q = 0.3$ (a) t=469 (maximum) (b) t=479 (minimum) (c) t=552 (maximum) (d) t=726 (minimum)

5 Conclusion

We have considered the numerical simulation of a convection roll between two differentially heated plates of small periodic dimensions. As the Rayleigh number increases, the convection roll shrinks and grows in a periodic, then quasi-periodic, then chaotic. For still higher values, the convection roll breaks down and reforms intermittently at another location. Lyapunov spectrum analysis was used to characterize the dynamical features of the flow. Two cases in the purely chaotic and intermittent regime were examined in detail. We found that although the asymptotic value of the largest exponent is positive, its most probable value is negative. We showed that intermittency corresponds to the occurence of higher positive values in the Lyapunov exponent corresponding

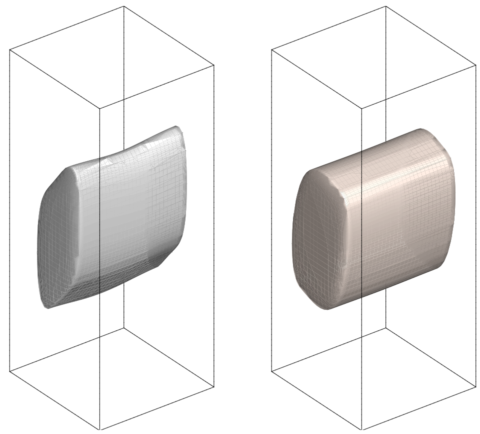

(a) (b)

Fig. 10. (Color online) Eigenvector associated with a local extremum of the short-time exponent at Ra = 12600 at the positions indicated in Figure 8 (b). Value of the Q isosurface (a) t=954 (maximum) $Q = 0.05$ (b) t=968 (minimum) $Q = 0.3$

to the break-up and reformation of the convection roll. The perturbations associated with the extremal values of the short-time largest exponent were identified. In the chaotic case, the perturbations associated with the largest extrema are 2D convection rolls. Maxima are associated with larger rolls, while minima are associated with less intense rolls. In the intermittent case, maxima were associated with a quasi 1-D flow, which corresponds to the break-up of the roll, while minima corresponded to 2D convection rolls and therefore the roll formation stage. These results confirm that the analysis of short-time Lyapunov exponents provides insight into the physics of the flow and suggests that it could be useful for low-order modelling of its complex dynamics.

References

1. P. Le Quéré. Onset of unsteadiness, routes to chaos and simulations of chaotic flows in cavities heated from the side: a review of present status. *10th Intl. Heat Trans. Conf.*, volume 1 of *I Chem E Symposium Series*, pages 281–296, 1994.
2. S. Paolucci and D.R. Chenoweth. Transition to chaos in a differentially heated vertical cavity. *J. Fluid Mech.*, 201:379–410, 1989.
3. T.A.M Versteegh and F.T.M. Nieuwstadt A direct numerical simulation of natural convection between two infinite vertical differentially heated walls scaling laws and wall functions *Int. J. Heat Mass Transfer*, 42:3673, 1999.
4. Z. Gao, A. Sergent, B. Podvin, S. Xin, P. Le Quéré, and L.S. Tuckerman. On the transition to chaos of natural convection between two infinite differentially heated vertical plates. *Phys. Rev. E*, 88:023010, Aug 2013.
5. J. L. Wright, H. Jin, K. G. T. Hollands, and D. Naylor. Flow visualization of natural convection in a tall, air-filled vertical cavity. *Int. J. Heat Mass Transfer*, 49:889–904, 2006.

6. Z. Gao, B. Podvin, A. Sergent, S. Xin, Chaotic dynamics of a convection roll in a highly cinfined, vertical, differentially heated fluid layer, submitted to Physical Reivew E.
7. S. Xin and P. Le Quéré. An extended Chebyshev pseudo-spectral benchmark for the 8:1 differentially heated cavity. *Int. J. Num. Meth. in Fluids*, 40:981–998, 2002.
8. G. Benettin, L. Galgani, A. Giorgilli and J. Strelcyn. Lyapunov characteristics exponents for smooth dynamical system and for hamiltonian system: a method for computing all of them. *Meccanica*, 15:9-30, 1980.
9. C.-M. Ho, and P. Huerre, Perturbed Free-shear Layers, *Annual Rev. Fluid Mech.* 1984, 16, 365-422.
10. L.S. Sirovich and A.E. Deane. A computational study of Rayleigh-Benard convection. part 2. dimension consideration. *J. Fluid Mech.*, 222:251-265, 1991.
11. E. Ott. *Chaos in Dynamical Systems.* Cambridge University Press, 2002.
12. G.A. Gottwald and I. Melbourne. A new test for chaos in deterministic systems. *Proc. R. Soc. Lond. A*, 460:603-611, 2004.
13. G.A. Gottwald and I. Melbourne. On the Implementation of the 0-1 Test for Chaos. *SIAM J. Appl. Dyn. Syst.*, 8(1):129-145, 1991.
14. T. Kapitaniak. Distribution of transient Lyapunov exponents of Quasiperiodically forced systems. *Prog. Theor. Phys.*, 93(4):831-833, 1995.
15. J.A. Vastano, R.D. Moser, Short-time Lyapunov exponent analysis and the transition to chaos in Taylor-Couette flow, *J. Fluid Mech.*, 233:83-118, 1991.